Note Added in Proof. The microwave structure of the C_2H_4/SO_2 complex has recently been determined.[35] It has a structure similar to the C_2H_4/O_3 complex,[30] where the two molecular planes are roughly parallel indicating an interaction between the π systems.

(35) LaBarge, M. S.; Hillig, K. W.; Kuczkowski, R. L. *Angew. Chem., Int. Ed. Engl.* **1988**, *27*, 1356.

Acknowledgment. We thank Dr. L. Thorne for suggesting this project and also Dr. D. Cremer and Prof. J. Almlöf for helpful conversations. M.L.M. was a participant in the Visiting Summer Faculty Program at Sandia National Laboratories, Livermore, while this work was performed. M.L.M. also thanks the donors of the Petroleum Research Fund, administered by the American Chemical Society, for financial support.

Registry No. PO, 6669-36-9; ethylene, 74-85-1.

Electronic Structure and Spectra of Uranocene

Agnes H. H. Chang and Russell M. Pitzer*

Contribution from the Department of Chemistry, The Ohio State University, 120 West 18th Avenue, Columbus, Ohio 43210. *Received August 3, 1988*

Abstract: The wave functions and energy levels for uranocene, $U(C_8H_8)_2$, have been computed using ab initio techniques including the spin-orbit interaction and relativistic core potentials. The results give detailed information on the bonding in the ground state and on the assignment of the visible spectrum. A large amount of mixing of the ligand π orbitals with the uranium 6d (and 5f) orbitals was found, confirming expectations of sizable covalent bonding. The symmetry of the ground state was found to be E_{3g}, in agreement with some previous experimental and theoretical results. There are many low-lying $5f^2$ excited states, only two of which have been observed, as well as $5f \rightarrow 6d$, $\pi \rightarrow 6d$, and $\pi \rightarrow 5f$ excited states. The visible bands, which give uranocene its green color, previously thought to be ligand-to-metal bands, are found to be primarily due to $5f \rightarrow 6d$ excitations. The basis set of 208 generally contracted Gaussian symmetry orbitals is of slightly better than double-ζ quality, and 32 carbon core electrons and 78 uranium core electrons were replaced by relativistic core potentials. Double-group symmetry-adapted configuration-interaction expansions up to 31 000 in length were used. Spin-orbit matrix elements were included in the Hamiltonian matrices.

Background. Uranocene, $U(C_8H_8)_2$, was first prepared by Streitwieser and Müller-Westerhoff[1] in 1968. One of their reasons for making this compound was that the uranium 5f orbitals might play a significant role in the metal-ligand bonding, analogous to the role of the iron 3d orbitals in ferrocene.

Uranocene is quite a stable compound and, as shown by X-ray crystallography,[2] has the anticipated "sandwich" structure. Its reactivity properties have been studied extensively[3-5] and many substituted uranocenes and other actinocenes have been synthesized.[4-8]

Uranocene's most distinctive physical properties are its paramagnetism and its green color.[1] Thus, its magnetic and spectroscopic properties have been studied extensively and, together with simple theoretical calculations, have yielded some information on its electronic states although this information is far from complete. In particular, the ground state of uranocene has not been conclusively assigned and the electronic spectra remain unassigned.

Theoretical Method. The accurate calculation of the electronic structure of molecules containing heavy atoms requires being able to deal not only with large numbers of electrons and the subtleties of electron correlation but also with the large magnitude of the spin-orbit effect and other relativistic effects. It has been shown that relativistically derived core potentials and spin-orbit operators provide a means by which all these difficulties can be addressed effectively.[9-13]

In this work the wave functions and energy levels for uranocene have been computed using these ab initio techniques. The many-electron wave functions were expanded in double-group symmetry-adapted functions. These configuration-interaction (CI) expansions are of modest length, but spin-orbit matrix elements were included in the corresponding Hamiltonian matrices.

Questions Studied. The theoretical results give information on several questions of basic interest to the electronic structure of uranocene. In particular, these include (1) the role of uranium orbitals in covalent bonding to the ligands, (2) the identification of the ground state, whether the weak field or strong field case applies and whether LS coupling or jj coupling applies, and (3) the assignment of the visible spectrum in terms of the nature of the excited states.

Previous Work

Preparation and Chemical Properties. In 1968, Streitwieser and Müller-Westerhoff[1] used potassium to generate $C_8H_8^{2-}$ ions in tetrahydrofuran solution and then added UCl_4 to prepare uranocene.

$$4K + 2C_8H_8 + UCl_4 \xrightarrow{THF} U(C_8H_8)_2 + 4KCl$$

Uranocene, when crystallized, is green, sublimes at 180 °C, and

(1) Streitwieser, A.; Müller-Westerhoff, U. *J. Am. Chem. Soc.* **1968**, *90*, 7364.
(2) Zalkin, A.; Raymond, K. N. *J. Am. Chem. Soc.* **1969**, *91*, 5667-5668.
(3) Streitwieser, A.; Müller-Westerhoff; Sonnichsen, U. G.; Mares, F.; Morrel, D. G.; Hodgson, K. O.; Harmon, C. A. *J. Am. Chem. Soc.* **1973**, *95*, 8644-8649.
(4) Marks, T. J.; Ernst, R. D. In *Comprehensive Organometallic Chemistry*; Wilkinson, G., Stone, F. G. A., Abel, E. W., Eds.; Pergamon: Oxford, 1982; Vol. 3, p 173-270.
(5) Streitwieser, A.; Kinsley, S. In *Fundamental and Technological Aspects of Organo-f-Element Chemistry*; Marks, T. J., Fragala, I. L., Eds.; Reidel: Dordrecht, Holland, 1985; pp 77-114.
(6) Karraker, D. G.; Stone, J. A.; Jones, E. R.; Edelstein, N. *J. Am. Chem. Soc.* **1970**, *92*, 4841-4845.
(7) Streitwieser, A.; Harmon, C. H. *Inorg. Chem.* **1973**, *12*, 1102-1104.
(8) Karraker, D. G. *Inorg. Chem.* **1973**, *12*, 1105-1108.
(9) Pitzer, K. S. *Int. J. Quantum Chem.* **1984**, *25*, 131-148.
(10) Krauss, M.; Stevens, W. J. *Annu. Rev. Phys. Chem.* **1984**, *35*, 357-385.
(11) Christiansen, P. A.; Ermler, W. C.; Pitzer, K. S. *Annu. Rev. Phys. Chem.* **1985**, *36*, 407-432.
(12) Balasubramanian, K.; Pitzer, K. S. *Adv. Chem. Phys.* **1987**, *67*, 287-319.
(13) Ermler, W. C.; Ross, R. B.; Christiansen, P. A. *Adv. Quantum Chem.* **1988**, *19*, 139-182.

0002-7863/89/1511-2500$01.50/0

is quite stable in oxygen-free environments.[1] Uranocene can even be made directly from C_8H_8 and metallic uranium.[14] Mass spectrometry[1] and X-ray crystallography[2,15] have shown that it has a sandwich structure with D_{8h} symmetry (site symmetry C_i in the crystal), and therefore it is an actinide analogue of ferrocene. The metal-ring bonds are quite strong in uranocene and even stronger when the ligands are substituted; the ligands are not easily displaced.[7]

Magnetic Properties. Crystal field theory, assuming the weak field case, gives $5f^2\ ^3H_4$ as the lowest term for uranocene; the D_{8h} symmetry ligand field splits the energy by $|M_J|$ values.[4,6,16] Karraker, Stone, Jones, and Edelstein[6] showed that the simplest range of choices of crystal field parameters gives $|M_J| = 4$, or possibly 0, as the ground state.

Magnetic susceptibility data have been obtained for uranocene from 1 to 298 K.[6,8,17,18] The data above 9 K fit the Curie–Weiss law fairly well, corresponding to effective magnetic moment values of 2.4 μ_B for lower temperatures and 2.6 μ_B at higher temperatures.[16] The value of 2.4 μ_B fits an $|M_J| = 3$ ground state or, with some difficulty, an $|M_J| = 4$ ground state.[6]

The magnetic susceptibility data below 9 K do not fit the Curie–Weiss law. An attempt to fit this behavior by assuming an $M_J = 0$ (nondegenerate) ground state has been made,[18] but this model required unobserved low-lying excited states and values of crystal field parameters inconsistent with other actinocenes.[16] Since some uranocene derivatives do not have this anomalous low-temperature behavior, it seems most likely that it is caused by small low-symmetry crystalline interactions.[16,17]

Dallinger, Stein, and Spiro[19] used a two-state fit for the magnetic susceptibility and obtained a best fit with $|M_J| = 4, 3$ for the ground and the first-excited states, respectively. Jahn, Yünlü, Oroschin, Amberger, and Fischer[20] tried several three-state fits to both the uranocene magnetic susceptibility data and the magnetic susceptibility anisotropy data for a uranocene derivative; their best fit was for ground state, first-excited state, and second-excited state $|M_J|$ values of 3, 2, 1.

Many ^{13}C and ^1H NMR studies on uranocene and its derivatives have been carried out,[17,20–23] and models of the spin densities in these molecules have been discussed extensively.[17,21,22,24,25] Since the chemical shifts in paramagnetic molecules must be separated into several terms in order to relate their values to the electronic structure, such calculations are difficult to parametrize. In detailed treatments, Fischer[25] and McGarvey[26] concluded that $|M_J| = 3$ fit better than $|M_J| = 4$ for the ground state of uranocene. Streitwieser[24] also noted that the ^{13}C chemical shifts indicate a large degree of charge transfer from the ligands to the uranium.

Thus, the magnetic properties of uranocene limit the choices in assigning the ground state and favor the $|M_J| = 3$ assignment but are not completely definitive in this regard.

Visible Spectrum. The characteristic green color of uranocene arises from a series of absorption bands which increase in intensity from low energy up to approximately 2 eV.[1,3,19,27] The three most intense bands are designated[19] I (2.017 eV), II (1.939 eV), and III (1.881 eV). Their intensities are too large for 5f → 5f transitions,[6] so they have usually been presumed to be $\pi \rightarrow$ 5f charge-transfer transitions. Electron-donating substituents cause small shifts to lower energy while electron-withdrawing substituents cause shifts to higher energy, and this behavior is consistent with these bands having charge-transfer character.[6,28] The intensity of band III shows a large temperature dependence, decreasing when the temperature is lowered,[27] so it is an electronic hot band.[19] Magnetic circular dichroism (MCD) spectroscopy has been used[27] to show that, taking the z axis to be 8-fold rotation axis, band I is z-polarized ($\Delta|M_J| = 0$) and band II is x,y-polarized ($\Delta|M_J| = \pm 1$).

Strong transitions have also been noted in the ultraviolet at 4.079 and 4.261 eV.[3]

Raman Spectra. Resonance Raman studies by Dallinger et al.[19] showed that a transition at 466 cm^{-1} (0.058 eV) is an electronic transition and polarization measurements showed that $\Delta|M_J| = \pm 1$ holds for this transition. They assigned it as 5f → 5f on the basis of its low energy and narrow width. Barron and Vrbancich[29] used magnetic electronic Raman spectroscopy on this transition to show that $\Delta|M_J| = -1$. It was assumed on the basis of magnetic susceptibility data[19,29] that the transition is 4 → 3 but the spectroscopic data support 3 → 2 equally well. Since the separation of visible bands II and III is also 0.058 eV, both bands have the same upper state and the temperature-dependent intensity of band III is due to its lower state being the 0.058-eV excited state.[19] Dallinger et al.[19] found band III to be z-polarized ($\Delta|M_J| = 0$) and verified the polarizations for bands I and II. Amberger[30] found another low-lying electronic state, presumed to be 5f → 5f as well, at 0.290 eV. It was characterized only by its lack of a thorocene analogue.

Photoelectron Spectra. He I photoelectron spectra of uranocene show low-energy peaks at 6.20, 6.90, and 7.85 eV.[31–33] By comparing intensities with the corresponding He II spectra, Clark and Green[33] assigned these as 5f, $e_{2u}(\pi)$, and $e_{2g}(\pi)$, respectively. Although the e_{2u} intensity comparison showed some admixture of 5f character into the ligand e_{2u} orbitals, the large e_{2u}–e_{2g} splitting indicated an even larger interaction between 6d orbitals and the ligand e_{2g} orbitals, suggesting that donation from the formal $C_8H_8^{2-}$ ligands to the U 6d orbitals is the principal covalent interaction.[33]

X-ray photoelectron spectra of uranocene show quite a low core ($4f_{7/2}$) binding energy and therefore a high degree of covalency in the bonding.[34] Comparison with the He photoelectron spectra of several uranium compounds suggests that the 5f orbitals in uranocene are principally nonbonding.[34]

Theoretical Calculations. Semiempirical molecular orbital calculations, both nonrelativistic[35] and relativistic[36] have been carried out on uranocene. These included only one-electron interactions and thus give information mainly about orbital mixing and orbital energies.

Ligand field theory calculations on uranocene have been carried out by Hayes and Edelstein[37] and by Warren.[38] Since this type of calculation includes all three of the basic interactions, mixing (interaction) of ligand and metal orbitals, electron repulsion, and spin–orbit, the results give information about the low-lying ($5f^2$)

(14) Starks, D. F.; Streitwieser, A. *J. Am. Chem. Soc.* **1973**, *95*, 3423–3424.
(15) Avdeef, A.; Raymond, K. N.; Hodgson, K. O.; Zalkin, A. *Inorg. Chem.* **1972**, *11*, 1083–1088.
(16) Warren, K. D. *Struct. Bonding (Berlin)* **1977**, *33*, 97–138.
(17) Edelstein, N.; LaMar, G. N.; Mares, F.; Streitwieser, A. *Chem. Phys. Lett.* **1971**, *8*, 399–402.
(18) Amberger, H.; Fischer, R. D.; Kanellakopulos, B. *Theor. Chim. Acta* **1975**, *37*, 105–127.
(19) Dallinger, R. F.; Stein, P.; Spiro, T. G. *J. Am. Chem. Soc.* **1978**, *100*, 7865–7870.
(20) Jahn, W.; Yünlü, K.; Oroschin, W.; Amberger, H.; Fischer, R. *Inorg. Chim. Acta* **1984**, *95*, 85–104.
(21) Streitwieser, A.; Dempf, D.; LaMar, G. N.; Karraker, D. G.; Edelstein, N. *J. Am. Chem. Soc.* **1971**, *93*, 7343–7344.
(22) Luke, W. D.; Streitwieser, A. In *Lanthanide and Actinide Chemistry and Spectroscopy*; Edelstein, N. M., Ed.; ACS Symposium Series 131; American Chemical Society: Washington, DC, 1980; p 93–140.
(23) McGarvey, B. R.; Nagy, S. *Inorg. Chem.* **1987**, *26*, 4198–4203.
(24) Streitwieser, A. In *Organometallics of the f-Elements*; Marks, T. J., Fisher, R. D., Eds.; Reidel: Dordrecht, Holland, 1979; pp 149–177.
(25) Fischer, R. D. In *Organometallics of the f-Elements*; Marks, T. J., Fischer, R. D., Eds.; Reidel: Dordrecht, Holland, 1979; pp 337–377.
(26) McGarvey, B. *Can. J. Chem.* **1984** *62*, 1349–1355.
(27) Mowery, R. L. Ph.D. Thesis, University of Virginia, 1976. *Diss. Abstr. Int.* **1977**, *37*, 5112B.
(28) Streitwieser, A. In *Topics in Nonbenzenoid Aromatic Chemistry*; Nozoe, T., Breslow, R., Hafner, K., Ito, S., Murata, I., Eds.; Hirokawa: Tokyo, 1973; Vol. 1, p 221–241.
(29) Barron, L. D.; Vrbancich, J. *J. Raman Spectrosc.* **1983**, *14*, 118–125.
(30) Amberger, H. *J. Less-Common Met.* **1983**, *93*, 235–236.
(31) Clark, J. P.; Green, J. C. *J. Organomet. Chem.* **1976**, *112*, C14–C16.
(32) Fragala, I.; Condorelli, G.; Zanella, P.; Tondello, E. *J. Organomet. Chem.* **1976**, *122*, 357–363.
(33) Clark, J. P.; Green, J. C. *J. Chem. Soc., Dalton Trans.* **1977**, 505–508.
(34) Beach, D. B.; Bomben, K. D.; Edelstein, N.; Eisenberg, D. C.; Jolly, W. L.; Shinomoto, R.; Streitwieser, A. *Inorg. Chem.* **1986**, *25*, 1735–1737.
(35) Fischer, R. D. *Theor. Chim. Acta* **1963**, *1*, 418–431.
(36) Pyykkö, P.; Lohr, L. L., Jr. *Inorg. Chem.* **1981**, *20*, 1950–1959.
(37) Hayes, R. G.; Edelstein, N. *J. Am. Chem. Soc.* **1972**, *94*, 8688–8691.
(38) Warren, K. D. *Inorg. Chem.* **1975**, *14*, 3095–3103.

Table I. Carbon and Uranium Basis Sets

orbital exponents	contraction coefficients		
	Carbon n = 1 Basis for 2s Orbitals		
25.04	−0.010 753 9		0.000 000 0
3.358	−0.137 415 3		0.000 000 0
0.4836	0.576 485 6		0.000 000 0
0.1519	0.535 644 4		1.000 000 0
	Carbon n = 2 Basis for 2p Orbitals		
9.43	0.038 152 1		0.000 000 0
2.001	0.209 455 4		0.000 000 0
0.5451	0.508 966 5		0.000 000 0
0.1516	0.468 378 9		1.000 000 0
	Uranium n = 3 Basis for 6s, 6d Orbitals		
2.168	−0.128 583 5	−0.019 626 9	0.000 000 0
1.008	0.795 938 0	−0.008 518 9	0.000 000 0
0.4017	0.364 515 3	0.527 674 6	0.000 000 0
0.1397	0.001 680 4	0.589 696 2	1.000 000 0
	Uranium n = 4 Basis for 6p, 5f Orbitals		
4.443	0.000 237 3	0.193 319 5	0.000 000 0
1.923	0.055 796 7	0.419 212 0	0.000 000 0
0.8641	0.663 238 9	0.395 460 8	0.000 000 0
0.3463	0.398 763 6	0.255 716 0	1.000 000 0

electronic states. Both calculations gave $|M_J| = 3, 2, 4$ for the ground, first-excited, and second-excited states, respectively. Neither calculation included 6d orbitals and neither gave direct information on the visible spectra.

Xα (muffin-tin) calculations, both nonrelativistic[39] and quasi-relativistic,[40,41] have been carried out on uranocene by Rösch and Streitwieser. An Xα (basis function) relativistic calculation has been carried out by Boerrigter, Baerends, and Snijders.[42] These confirmed the assignment of the He photoelectron spectra, the importance of the 6d orbitals in bonding, and the large amount of ligand-to-metal charge transfer. Since Xα calculations determine the molecular orbitals but not how they are coupled together, they do not directly give the symmetry of the ground state and only give crude information on the visible spectrum.

Theoretical Procedures

Geometry. Bond lengths of U–C = 2.647 Å, C–C = 1.392 Å, and C–H = 1.090 Å together with D_{8h} symmetry were used to determine the coordinates for each nucleus. The U–C and C–C bond lengths are X-ray crystallographic values;[15] the C–H bond length was not determined in the crystal structure, so a standard value was used.

Electron Configuration. The ground-state electron configuration for uranocene is most easily obtained by considering the molecule to be $U^{4+}(C_8H_8^{2-})_2$. The ligands then have closed shells; U has the electron configuration (closed shells) $5f^36d^17s^2$ so U^{4+} has (closed shells) $5f^2$. Thus uranocene also has the electron configuration (closed shells) $5f^2$. For this electron configuration there are 7 open-shell orbitals, 14 open-shell spin orbitals, and 91 overall wave functions; with D_{8h} double-group symmetry, there are 58 different energies.

Core Potential Method. Effective core potentials are obtained by standard procedures from relativistic atomic calculations;[11] effective spin–orbit operators are obtained simultaneously. The resulting valence pseudoorbitals have the same energies as the valence orbitals but only require basis functions for the valence region. The molecular (nonrelativistic) Schrödinger equation is solved for the valence electrons by replacing the core electrons with the effective core potentials. Hence, the core region of the molecule, including the inner parts of the valence orbitals, is treated relativistically and the valence region is treated nonrelativistically except that the spin–orbit interaction is included.

Core Potentials, Spin–Orbit Operators, and Basis Sets. The core potentials and spin-orbit operators for carbon are from Pacios and Christiansen;[43] the 1s shell is the core, and the 2s and 2p are valence shells. Those for uranium are from Christiansen;[44] 1s through 5d are in the core, and 6s, 6p, 5f, 6d, and 7s are valence shells. Generally contracted Gaussian atomic orbital (AO) basis sets were used for hydrogen, carbon, and uranium: H, (4s) → [2s]; C, (4s4p) → [2s2p]; U, (4ds4fp) → [3ds3fp]. The hydrogen set is from van Duijneveldt[45] and was scaled as recommended by Dunning.[46] The carbon and uranium sets were obtained by using a core-potential atomic self-consistent-field (SCF) program to optimize the orbital exponents. The C and U basis sets are listed in Table I.

The (4ds4fp) notation means that the d and s exponents were constrained to be the same, as were the f and p exponents. The principal quantum numbers were 3 for d, s and 4 for f, p. The advantages of this type of basis are, first, the number of basis functions is reduced since molecular integral programs use Cartesian Gaussians where 3s and 3d, 4p and 4f are combined, and, second, using 3s functions instead of 1s and 4p instead of 2p makes it easier to describe valence pseudoorbitals, which go to zero rapidly in the core region, as required.[43]

Use of the C and U core potentials removed 32 and 78 electrons from the calculations, respectively. The basis set of 208 generally contracted Gaussian AOs was used for the 94 valence electrons in uranocene.

Table II. Computer Time[a]

ARGOS	55	LSTRN	6
CNVRT	5	CIGNLS	0.2
SCF	7	CIDG	24

[a] Cray X-MP CPU time in minutes.

Computer Program and Resources. The Cray- X-MP central processor (CPU) time for each step of the calculation is shown in Table II.

All the molecular integrals are computed over symmetry orbitals using the ARGOS (Argonne, Ohio State) program.[47] In addition to AO overlap, kinetic energy, nuclear attraction, and electron repulsion integrals,[48] AO core potential integrals[49,50] and spin–orbit integrals[50] are evaluated. Since ARGOS was originally designed to be used with configuration–interaction programs for which the use of point-group symmetry higher than D_{2h} is difficult, only D_{2h} symmetry was used in the computations; all of the wave functions have D_{8h} symmetry, however, and D_{8h} notation is used in describing the results of the calculations.

The 3×10^7 integrals computed required approximately 60 megawords of disk space.

P and K supermatrix integrals are formed[51] from the electron repulsion integrals in order to carry out restricted Hartree–Fock SCF calculations.[52] In addition, improved virtual orbital (IVO) calculations[52,53] are carried out in order to obtain better orbitals for excited states of the molecule.

The integrals from ARGOS, including spin–orbit integrals, are transformed[54] into integrals over molecular orbitals according to each set of IVO molecular orbital coefficients. The only molecular orbital integrals retained are those over active orbitals (involved in the CI). The (spatial) electron configurations used in the CI calculations are generated[55] by excitations from a specified list of reference electron configurations. The number of open-shell orbitals and the parity are kept consistent with the overall double-group symmetry.

(39) Rösch, N.; Streitwieser, A. *J. Organomet. Chem.* **1978**, *145*, 195–200.
(40) Rösch, N.; Streitwieser, A. *J. Am. Chem. Soc.* **1983**, *105*, 7237–7240.
(41) Rösch, N. *Inorg. Chim. Acta* **1984**, *94*, 297–299.
(42) Boerrigter, P. M.; Baerends, E. J.; Snijders, J. G. *Chem. Phys.* **1988**, *122*, 357–374.
(43) Pacios, L. F.; Christiansen, P. A. *J. Chem. Phys.* **1985**, *82*, 2664–2671.
(44) Christiansen, P. A., private communication.
(45) van Duijneveldt, F. B. Technical Research Report No. RJ945; IBM: 1971.
(46) Dunning, T. H. *J. Chem. Phys.* **1970**, *53*, 2823–2833.
(47) Pitzer, R. M. (principal author). This program evolved from an earlier program written by H. L. Hsu and R. M. Pitzer. ARGOS is part of the COLUMBUS suite of programs. See: Shepard, R.; Shavitt, I.; Pitzer, R. M.; Comeau, D. C.; Pepper, M.; Lischka, H.; Szalay, P. G.; Ahlrichs, R.; Brown, F. B.; Zhao, J. G. *Int. J. Quantum Chem., Quantum Chem. Symp.* **1988**, *22*, 149–165. The general-contraction transformations use established methods: Raffenetti, R. C. *J. Chem. Phys.* **1973**, *58*, 4452–4458. The overall structure of the program and the symmetry algorithms are based on equal-contributions analysis: Pitzer, R. M. *J. Chem. Phys.* **1973**, *58*, 3111–3112.
(48) Dupuis, M.; Rys, J.; King, H. F. *J. Chem. Phys.* **1976**, *65*, 111–116.
(49) McMurchie, L. E.; Davidson, E. R. *J. Comput. Phys.* **1981**, *44*, 289–301.
(50) Pitzer, R. M.; Winter, N. W., paper in preparation.
(51) Yamaguchi, Y.; Brooks, B. CNVRT Modified by: Brown, F. B.; Pitzer, R. M.
(52) SCF, written, modified, and enhanced by a multitude of people at Argonne National Laboratory, Iowa State University, and The Ohio State University. See: Hsu, H. L.; Pitzer, R. M.; Davidson, E. R. *J. Chem. Phys.* **1976**, *65*, 609–613. Pitzer, R. M. OSU–TCG Report No. 101, unpublished.
(53) Hunt, W. J.; Goddard, W. A. *Chem. Phys. Lett.* **1969**, *3*, 414–418.
(54) LSTRN, modified from CITRAN by R. M. Pitzer: Brown, F. B. Ph.D. Thesis, The Ohio State University, 1982. *Diss. Abstr. Int.* **1983**, *43*, 3253B.
(55) CIGNLS, modified from MQM23 by R. M. Pitzer and N. W. Winter: Olafson, B. D.; Ladner, R. C. California Institute of Technology. See also ref 59.

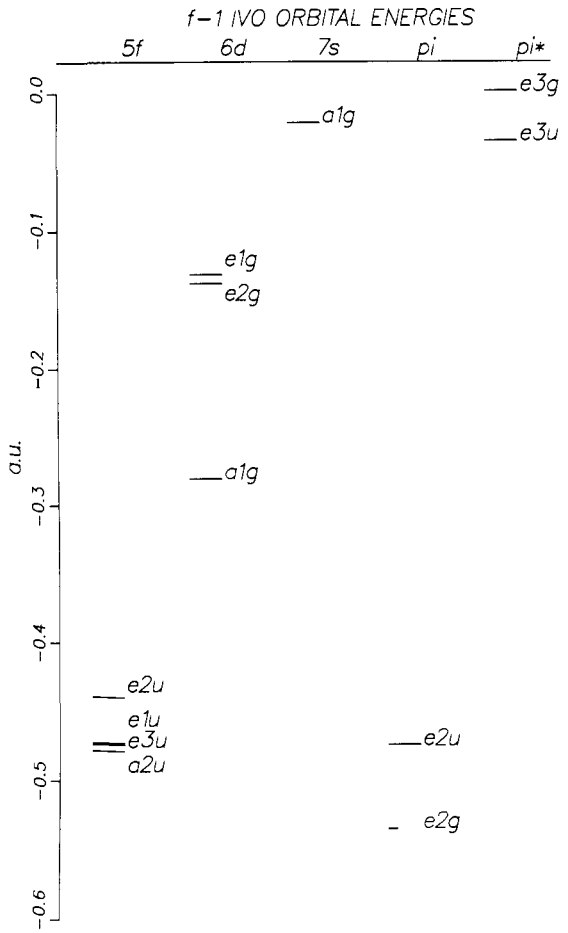

Figure 1. f^{-1} orbital energies.

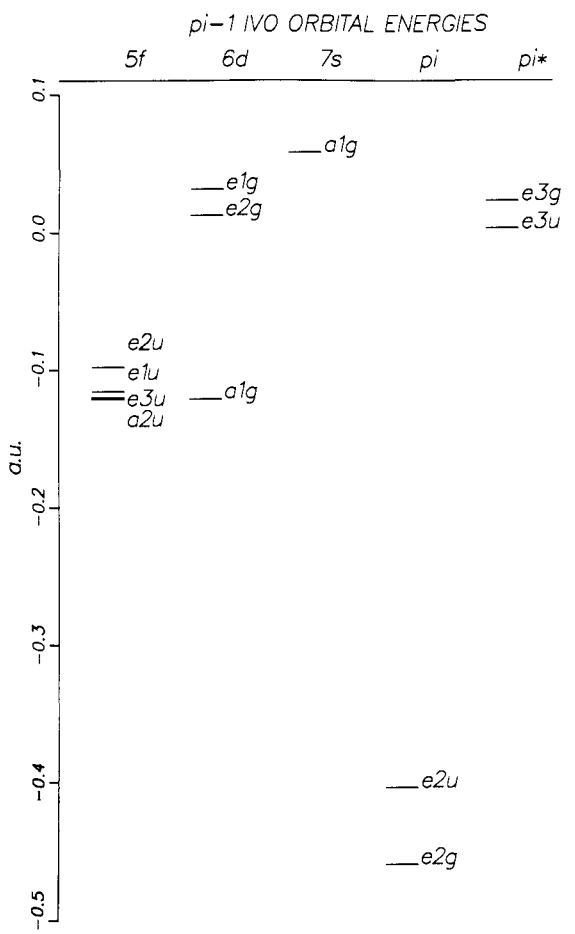

Figure 2. π^{-1} orbital energies.

The spin-orbit configuration-interaction program, CIDG,[56] starts with the MO integrals and the configuration lists. For each electron configuration, all Slater determinants[57,58] and double-group functions[59] are defined which are consistent with the overall symmetry of the state. Each block of matrix elements is formed over determinants[58] and then transformed to double-group functions.[59] Algorithms based on double-group properties are used to keep the Hamiltonian matrix real.[59] The energy eigenvalues and CI eigenvectors are obtained[60] with a simultaneous multiroot overrelaxation algorithm.[60,61] The number of configurations that can be used is much smaller than can be used with direct CI methods.

Results and Discussion

Molecular Orbitals. In order to have one set of molecular orbitals to use in CI calculations for all f^2 states, the average energy of all the f^2 states was used in the SCF calculation, i.e. the average energy of all 91 wave functions.

For excited states involving an excitation from the 5f shell, an IVO calculation was carried out in which the unoccupied orbitals were determined by the potential of the frozen occupied orbitals with a hole in the 5f shell. Similarly, unoccupied orbitals for excited states involving an excitation from the ligand π shells were determined using a hole averaged over these shells. These sets of orbitals are designated f^{-1} and π^{-1}, respectively.

Only 21 molecular orbitals were chosen as active orbitals in the spin-orbit CI calculation: U, 5f, 7; U, 6d, 5; U, 7s, 1; C_8H_8, π, 4; C_8H_8, π^*, 4. The other 42 occupied orbitals were frozen in the CI, and the higher energy virtual orbitals were eliminated.

Table III. Orbital Energies[a]

orbitals	f^{-1} IVO	π^{-1} IVO	SCF
e_{3g} (π^*)	0.001 467	0.022 968	0.193 134
a_{1g} (7s)	−0.021 174	0.058 707	0.409 126
e_{3u} (π^*)	−0.034 014	0.002 638	−0.017 639
e_{1g} (6d)	−0.131 861	0.032 290	0.225 361
e_{2g} (6d)	−0.138 142	0.012 941	0.212 841
a_{1g} (6d)	−0.279 974	−0.120 863	0.081 836
e_{2u} (5f)	−0.439 456	−0.097 029	−0.395 733
e_{1u} (5f)	−0.472 357	−0.114 579	−0.426 928
e_{2u} (π)	−0.472 807	−0.402 315	−0.246 214
e_{3u} (5f)	−0.473 476	−0.119 512	−0.428 379
a_{2u} (5f)	−0.477 964	−0.120 529	−0.432 589
e_{2g} (π)	−0.533 245	−0.457 595	−0.298 528

[a] Energy in atomic units.

Table IV. Population Analysis

1. Atomic Charges

atom	charge	atom	charge
H	+0.22	U	+0.98
C	−0.28		

2. Uranium Orbitals: Donation from Ligands

orbital	no. of electrons	orbital	no. of electrons
7s	0.43	6d	1.98
7p	0.11	5f	0.50

Orbital Energies. Figure 1 shows the orbital energies of the active orbitals for the IVO f^{-1} calculation. The order of orbital energies within the ligand π orbitals, i.e. $e_{2u} > e_{2g}$ (and $e_{1u} > e_{1g}$, not shown), is in agreement with the photoelectron studies[33] and Xα and other calculations.[36,39,40,42] The $f_{\pm 2}$ (e_{2u}) orbital energy

(56) Written by R. M. Pitzer and N. W. Winter using sections from programs developed at the California Institute of Technology, Los Alamos National Laboratory, Lawrence Livermore National Laboratory, and The Ohio State University. See ref 57–60.
(57) Ladner, R. C. Ph.D. Thesis, California Institute of Technology, 1972. *Diss. Abstr. Int.* **1972**, *33*, 1036B.
(58) Bobrowitz, F. W. Ph.D. Thesis, California Institute of Technology, 1974. *Diss. Abstr. Int.* **1974**, *35*, 2058B.
(59) Pitzer, R. M.; Winter, N. W. *J. Phys. Chem.* **1988**, *92*, 3061–3063.
(60) Shavitt, I. NASA-Ames Report, 1977, unpublished.
(61) Raffenetti, R. C. *J. Comput. Phys.* **1979**, *32*, 403–419.

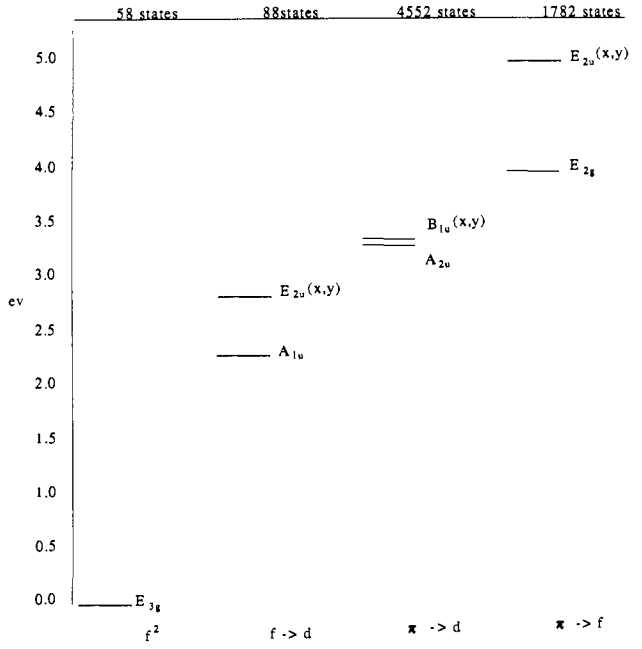

Figure 3. Lowest state and lowest allowed state (if any) for each class of states.

is the highest of the 5f orbitals, in agreement with other theoretical work.[37-40,42]

The IVO π^{-1} orbital energies are shown in Figure 2, in which the order within the 5f, 6d, π, and π^* orbitals is the same as in the IVO f^{-1} calculation, but the order between these groups of orbitals is somewhat different. The values of orbital energies obtained from the two IVO calculations and the SCF calculation are given in Table III.

Since the SCF calculation used the average energy of all $5f^2$ states, the orbital energies are less significant than they would be in calculations on individual states.

Population Analysis and Bonding. The Mulliken population analysis from the SCF calculation is shown in Table IV, and care should be taken to avoid too detailed an interpretation since the values are moderately basis set dependent. The calculated charge on uranium being only +0.98 rather than the formal +4 suggests that ligand-to-metal donation and therefore covalent bonding is very important. The distribution of electrons accumulated in the uranium atomic orbitals, 0.43 in 7s, 0.11 in 7p, 1.98 in 6d, and 2.50 in 5f, shows the primary role of the 6d orbitals in the bonding. Improvements in the basis set would surely reduce the amount of donation since negatively charged species such as $C_8H_8^{2-}$ are more sensitive to basis set quality than are positively charged species such as U^{4+}. Perhaps the most significant number is the relative amount of donation to d and f orbitals, 1.98 in 6d vs 0.50 in 5f. The population analysis results of Boerrigter et al.,[42] expressed as comparably as possible, give 0.94 in 6d and 0.71 in 5f for donation from the ligands, which indicates a more equal bonding role for the 6d and 5f orbitals. Photoelectron spectra[33] and Xα (muffin-tin) calculations[39,40] also indicate that the 6d orbitals are important in bonding.

Excited-State Calculations. Figure 3 shows the lowest and lowest dipole-allowed electronic states of uranocene for each of the following types of excitation: f → f, f → d, π → d, π → f. The energy range is up to 5 eV above the ground-state (E_{3g}) energy.

These results are from spin–orbit CI calculations with up to 2200 singly excited double-group-adapted functions using the f^{-1} orbitals. Only 10 of the valence electrons, 8 in the highest occupied ligand π orbitals and 2 in the uranium 5f orbitals, were active in the CI; the other 84 valence electrons were kept frozen. All configurations with one of the 5f electrons excited to 6d, 7s, or π^* MOs, or one of the π electrons excited to 5f, 6d, 7s, or π^* MOs were included.

Symmetry Notation. Once spin–orbit terms are included in the Hamiltonian, neither spatial symmetry operators nor spin angular momentum operators commute with the Hamiltonian. Symmetry operators which operate on both space and spin coordinates may still commute with the Hamiltonian, however, and the group of such operators is the double group. Its irreducible representations then designate the combined spatial and spin symmetry properties of the wave functions.

The correspondence between crystal field notation and notation for D_{8h} double-group (D_{8h}') irreducible representations is shown below for f^2 $^3H_4$ states:

crystal field	D_{8h}'
$M_J = 0$	A_{1g}
$\|M_J\| = 1$	E_{1g}
$\|M_J\| = 2$	E_{2g}
$\|M_J\| = 3$	E_{3g}
$\|M_J\| = 4$	$B_{1g} + B_{2g}$

For odd J values the $M_J = 0$ state is A_{2g}. For electron configurations with odd parity the g subscripts are changed to u subscripts.

Ground State. As Figure 3 shows, the ground state of uranocene has symmetry E_{3g} ($|M_J| = 3$), in agreement with previous calculations[37,38] and most, but not all, conclusions drawn from magnetic data. It is interesting that although the 6d orbitals play the dominant role in covalent bonding to the ligands, it is the smaller such role of the 5f orbitals that determines which state is the ground state.

The $f_{\pm 2}$–ligand–π interaction, in raising the energy of the $f_{\pm 2}$ orbitals, also raises the energy of f^2 wave functions according to their $f_{\pm 2}$ population.[42] The $f_{\pm 2}$ population of atomic f^2 $^3H_4$ wave functions is the least for $|M_J| = 3$ and increases in the order $|M_J| = 2, 1, 0, 4$.

Despite the limited nature of the CI calculations, it seems quite unlikely that any other state could be the ground state. The only alternative at all consistent with the magnetic susceptibility data is the slightly split $|M_J| = 4$ pair of states, which are computed to be the second and third excited states; they are at considerably higher energy than the first excited state. It is evident that calculations that treat, even quite approximately, the ligand interaction (including π-5f mixing), electron repulsion, and spin–orbit all give the E_{3g} result.

Coupling Description. The absolute squares of the ground state, E_{3g}, CI coefficients for the f^2 configurations are compared with their pure LS and jj coupling values in Table V. Due to the ligand-π interaction raising the energy of the $f_{\pm 2}$ (e_{2u}) orbitals, the triplet terms containing $f_{\pm 2}$ (e_{2u}) have coefficients lower than those for either pure coupling case; this represents a deviation from the weak-field approximation. Since the CI coefficients are normalized, other coefficients are correspondingly larger than those for either pure coupling case. The extent of deviation from LS coupling is best shown by the coefficient for the $e_{3u}a_{2u}$ ($S = 0$) term, which is of moderate size compared to the jj coupling value. Thus, there are significant deviations from the weak-field, LS-coupling model, but it is still the best simple description. Better values for these CI coefficients could probably be obtained from a spin–orbit MCSCF calculation.

Table V. $U(C_8H_8)_2$ Ground-State Wave Function Composition

configuration	LS coupling (f^2, $^3H_4$, $\|M_J\| = 3$)	jj coupling ($f_{5/2}^2$, $J = 4$, $\|M_J\| = 3$)	computed E_{3g}
$e_{3u}e_{1u}$ ($S = 1$)	0.673	0.490	0.680
$e_{3u}a_{2u}$ ($S = 1$)	0.194	0.184	0.227
$e_{3u}a_{2u}$ ($S = 0$)	0.000	0.184	0.053
$e_{2u}e_{1u}$ ($S = 1$)	0.097	0.041	0.023
$e_{2u}a_{2u}$ ($S = 1$)	0.036	0.061	0.011
$e_{2u}e_{1u}$ ($S = 0$)	0.000	0.041	0.006

[a] f_0, a_{2u}; $f_{\pm 1}$, e_{1u}; $f_{\pm 2}$, e_{2u}; $f_{\pm 3}$, e_{3u}.

f → f States. The lowest energy f → f (or f^2) states are shown in Figure 4. The Raman transition to the first excited state, 466 cm^{-1} (0.058 eV), $\Delta|M_J| = -1$,[19,29] corresponds to the calculated results of 0.109 eV, E_{3g} ($|M_J| = 3$) → E_{2g} ($|M_J| = 2$). The second Raman transition at 0.290 eV[30] corresponds to excitation to the slightly split B_{1g}, B_{2g} pair of states calculated at 0.364 and 0.360

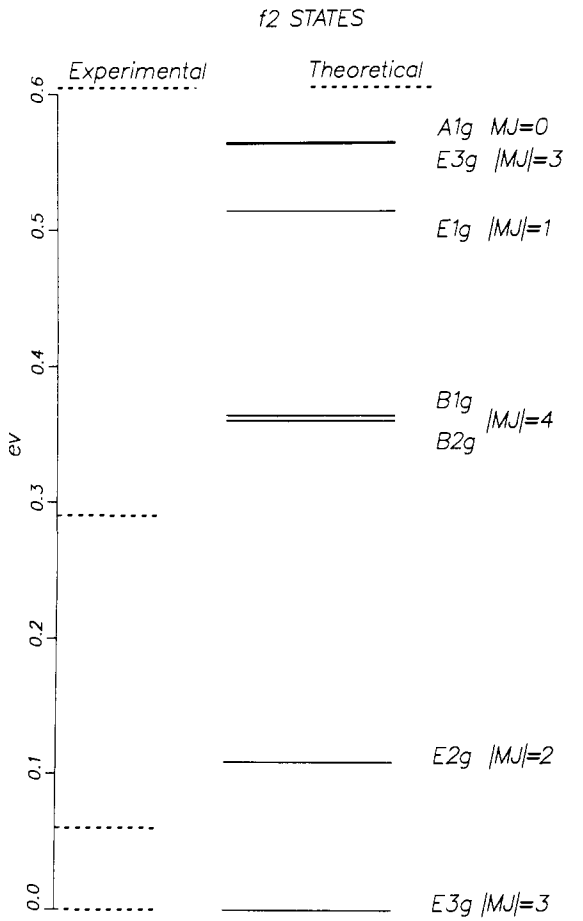

Figure 4. Lowest f^2 states.

Table VI. Excited-State Wave Function Composition

E_{3u} ($f \rightarrow d$, 2.905 eV)		
$e_{2g}(\pi)^4e_{2u}(\pi)^4a_{1g}(d)^1e_{3u}(f)^1$	S = 1	0.396
	S = 0	0.184
$e_{2g}(\pi)^4e_{2u}(\pi)^3a_{1g}(d)^1e_{3u}(f)^1e_{2u}(f)^1$	S = 0, 1, 2	0.237
E_{2u} ($f \rightarrow d$, 2.837 eV)		
$e_{2g}(\pi)^4e_{2u}(\pi)^4a_{1g}(d)^1e_{3u}(f)^1$	S = 1	0.593
$e_{2g}(\pi)^4e_{2u}(\pi)^3a_{1g}(d)^1e_{2u}(f)^1e_{3u}(f)^1$	S = 1, 2	0.237
A_{1u} ($f \rightarrow d$, 2.280 eV)		
$e_{2g}(\pi)^4e_{2u}(\pi)^4a_{1g}(d)^1a_{2u}(f)^1$	S = 1	0.402
$e_{2g}(\pi)^4e_{2u}(\pi)^4a_{1g}(d)^1e_{1u}(f)^1$	S = 1	0.192
$e_{2g}(\pi)^3e_{2u}(\pi)^3a_{1g}(d)^1e_{2u}(f)^1a_{2u}(f)^1$	S = 1, 2	0.173
B_{1g} (f^2, 0.364 eV)		
$e_{2g}(\pi)^4e_{2u}(\pi)^4e_{3u}(f)^1e_{1u}(f)^1$	S = 1	0.707
$e_{2g}(\pi)^4e_{2u}(\pi)^4a_{2u}(f)^1e_{3u}(f)^1$	S = 1	0.135
B_{2g} (f^2, 0.360 eV)		
$e_{2g}(\pi)^4e_{2u}(\pi)^4e_{3u}(f)^1e_{1u}(f)^1$	S = 1	0.707
$e_{2g}(\pi)^4e_{2u}(\pi)^4a_{2u}(f)^1e_{3u}(f)^1$	S = 1	0.135
E_{2g} (f^2, 0.109 eV)		
$e_{2g}(\pi)^4e_{2u}(\pi)^4a_{2u}(f)^1e_{3u}(f)^1$	S = 1	0.660
$e_{2g}(\pi)^4e_{2u}(\pi)^4e_{3u}(f)^1e_{1u}(f)^1$	S = 1	0.148

eV. The set of states corresponding to $^3H_4$ ($|M_J| = 0$–4) is apparent in Figure 4 and has a slight overlap with the next set of states. The main configurations, with the fractional contributions to the wave functions, of the E_{2g}, B_{2g}, and B_{1g} states are listed in Table VI. The principal configurations for the B_{2g} and B_{1g} states indicate appreciable mixing with $^3H_5$ wave functions, evidence of deviation from the weak-field approximation. Below 2.280 eV, the location of the first $f \rightarrow d$ state, there are 38 f^2 states; they are listed in Table VII.

$f \rightarrow d$ States. The lowest energy $f \rightarrow d$ (or fd) states are shown in Figure 5, and the energy values are given in Table VIII. The two lowest energy states, A_{1u} at 2.280 eV and E_{1u} at 2.385 eV,

Table VII. First 38 f^2 States

	state	energy, eV		state	energy, eV
38	E_{1g}	2.189	19	E_{1g}	1.234
37	A_{1g}	2.187	18	A_{1g}	1.153
36	E_{3g}	2.122	17	B_{1g}	1.121
35	E_{2g}	1.999	16	B_{2g}	1.118
34	A_{1g}	1.873	15	E_{2g}	1.111
33	E_{2g}	1.869	14	A_{2g}	1.090
32	E_{2g}	1.856	13	E_{3g}	0.999
31	E_{1g}	1.811	12	E_{3g}	0.844
30	E_{3g}	1.741	11	B_{2g}	0.816
29	B_{2g}	1.688	10	B_{1g}	0.811
28	A_{2g}	1.680	9	E_{2g}	0.773
27	B_{1g}	1.679	8	E_{1g}	0.754
26	E_{2g}	1.538	7	A_{1g}	0.565
25	E_{3g}	1.533	6	E_{3g}	0.564
24	E_{1g}	1.504	5	E_{1g}	0.514
23	E_{1g}	1.474	4	B_{1g}	0.364
22	E_{3g}	1.425	3	B_{2g}	0.360
21	E_{2g}	1.388	2	E_{2g}	0.109
20	A_{1g}	1.351	1	E_{3g}	0.000

Table VIII. $f \rightarrow d$ States[a]

state	excitation energy, eV	electric dipole transition	state	excitation energy, eV	electric dipole transition
A_{1u}	3.211	forbidden	A_{2u}	2.893	forbidden
E_{1u}	3.091	forbidden	E_{2u}	2.837	allowed (x, y)
E_{2u}	2.961	allowed (x, y)	E_{1u}	2.385	forbidden
E_{3u}	2.905	allowed (z)	A_{1u}	2.280	forbidden

[a] Six f^2 states also in this energy range.

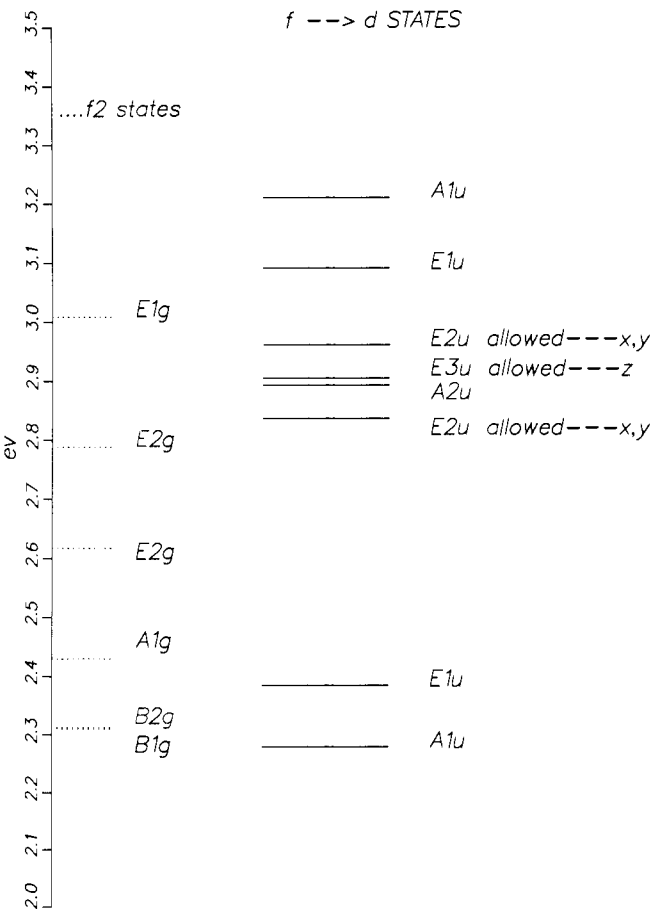

Figure 5. Lowest $f \rightarrow d$ states.

are not electric dipole allowed from the ground state although E_{1u} is allowed from the E_{2g} state (x,y-polarized). The first allowed transition from the ground state is to an $f \rightarrow d$ E_{2u} state at 2.837 eV (x,y-polarized); the second allowed transition is to an $f \rightarrow d$

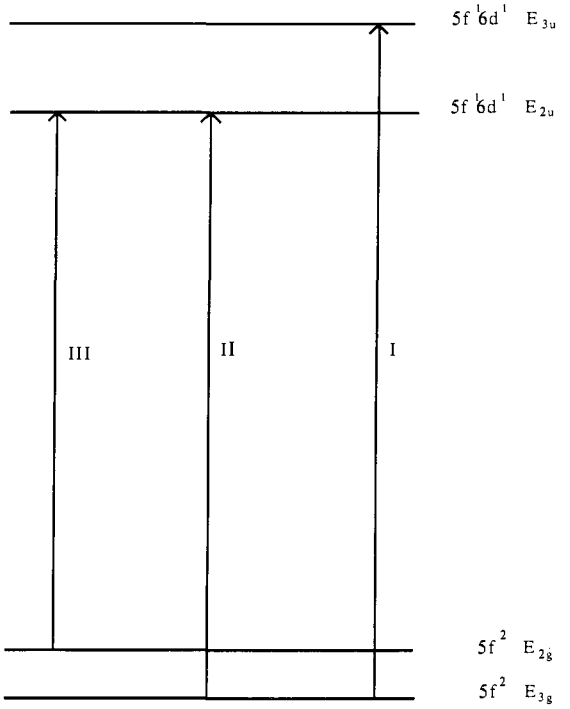

Figure 6. Transitions in visible spectrum.

E_{3u} state at 2.905 eV (z-polarized).

The E_{2u} and E_{3u} states provide a consistent assignment for the upper states for the visible spectrum: band I, $E_{3g} \rightarrow E_{3u}$, 2.905 eV calculated, 2.017 eV measured, z-polarized; band II, $E_{3g} \rightarrow E_{2u}$, 2.837 eV calculated, 1.939 eV measured, x,y-polarized; band III, $E_{2g} \rightarrow E_{2u}$, 2.728 eV calculated, 1.881 eV measured, z-polarized. A diagram of these transitions is shown in Figure 6. The x,y-polarized, not experimentally measured, $E_{2g} \rightarrow E_{3u}$ transition, calculated to be at 2.796 eV, expected experimentally at 1.959 eV, may be buried under band II. The calculated order of the bands and their polarizations are correct, and their spacings agree moderately, but they are all about 0.9 eV too high. This error is not particularly surprising in view of the limited number of active orbitals and the limited length of the CI expansions.

Thus, the visible bands, previously suggested to be ligand-to-metal $\pi \rightarrow$ f charge-transfer transitions, are found to be f $\rightarrow$ d transitions. The CI coefficients show a moderate amount of mixing of $\pi \rightarrow$ d character into these wave functions: between 29% and 40% for the E_{2u} and E_{3u} states. The fraction of $\pi \rightarrow$ d character may be sensitive to improvements in the wave functions. The main configurations of the A_{1u}, E_{2u}, and E_{3u} wave functions are given in Table VI along with their fractional contributions to the wave functions. The partial charge-transfer character of these states is probably sufficient to explain the observed shifts of the visible bands to lower energy in derivatives containing electron-donating substituents.[7,28]

There are a total of 140 f $\rightarrow$ d wave functions, forming 88 states of which 49 are allowed from the ground state. Only 8 of these states, 3 of them allowed, lie below the lowest state of mainly charge-transfer (π excitation) character.

$\pi \rightarrow$ d and $\pi \rightarrow$ f States. The first predominantly charge-transfer state, a $\pi \rightarrow$ d ($e_{2g}(\pi)^4e_{2u}(\pi)^3f^2d$) A_{2u} state, occurs at 3.311 eV. The first electric-dipole-allowed charge-transfer state is a $\pi \rightarrow$ d B_{1u} state (x,y-polarized) and is at 3.322 eV. The first $\pi \rightarrow$ f state, an ($e_{2g}(\pi)^4e_{2u}(\pi)^3f^3$) E_{2g} state, occurs at 3.954 eV. The first electric-dipole-allowed $\pi \rightarrow$ f state, an E_{2u} state (x,y-polarized), lies at 5.012 eV. Since the e_{2g} (π) MOs lie significantly lower than the e_{2u} (π) MOs, the lower $\pi \rightarrow$ d states are u and the lower $\pi \rightarrow$ f states are g.

There are a total of 7280 $\pi \rightarrow$ d wave functions, forming 4552 states of which 1365 are allowed from the grond state, and there are 2912 $\pi \rightarrow$ f wave functions, forming 1782 states of which 546 are allowed from the ground state. Many of these excited-state wave functions involve a different coupling of the 5f electrons than the ground state and are therefore expected to have low intensities. A list of dipole-allowed f $\rightarrow$ d and $\pi \rightarrow$ d states with calculated excitation energies up to 3.8 eV is given in Table IX.

Table IX. $U(C_8H_8)_2$ Dipole-Allowed States

state	ΔE, eV	character	polarization	state	ΔE, eV	character	polarization
B_{2u}	3.814	$\pi \rightarrow$ d	x, y	E_{2u}	3.484	$\pi \rightarrow$ d	x, y
B_{1u}	3.802	$\pi \rightarrow$ d	x, y	E_{3u}	3.477	f $\rightarrow$ d	z
E_{3u}	3.796	$\pi \rightarrow$ d	z	E_{3u}	3.395	$\pi \rightarrow$ d	z
E_{3u}	3.769	$\pi \rightarrow$ d	z	B_{1u}	3.377	f $\rightarrow$ d	x, y
B_{2u}	3.737	$\pi \rightarrow$ d	x, y	B_{2u}	3.377	f $\rightarrow$ d	x, y
B_{1u}	3.735	$\pi \rightarrow$ d	x, y	E_{3u}	3.349	$\pi \rightarrow$ d	z
E_{2u}	3.693	$\pi \rightarrow$ d	x, y	B_{2u}	3.327	$\pi \rightarrow$ d	x, y
E_{3u}	3.565	$\pi \rightarrow$ d	z	B_{1u}	3.322	$\pi \rightarrow$ d	x, y
E_{3u}	3.557	$\pi \rightarrow$ d	z	E_{2u}	2.961	f $\rightarrow$ d	x, y
E_{2u}	3.554	$\pi \rightarrow$ d	x, y	E_{3u}	2.905	f $\rightarrow$ d	z
E_{2u}	3.522	$\pi \rightarrow$ d	x, y	E_{2u}	2.837	f $\rightarrow$ d	x, y
B_{2u}	3.491	$\pi \rightarrow$ d	x, y	E_{3g}	0.00	f^2	
B_{1u}	3.490	$\pi \rightarrow$ d	x, y				

Table X. Electronic Energies Calculated with f^{-1} and π^{-1} Orbitals

character	states	f^{-1}, eV	π^{-1}, eV	character	states	f^{-1}, eV	π^{-1}, eV
$\pi \rightarrow$ d	B_{2u}	3.327	3.144	f^2	A_{1g}	0.565	0.552
$\pi \rightarrow$ d	B_{1u}	3.322	3.140	f^2	E_{3g}	0.564	0.561
$\pi \rightarrow$ d	A_{2u}	3.311	3.130	f^2	E_{1g}	0.514	0.510
f $\rightarrow$ d	E_{3u}	2.905	2.733	f^2	B_{1g}	0.364	0.361
f $\rightarrow$ d	E_{2u}	2.837	2.674	f^2	B_{2g}	0.360	0.357
f $\rightarrow$ d	E_{1u}	2.385	2.315	f^2	E_{2g}	0.109	0.111
f $\rightarrow$ d	A_{1u}	2.280	2.232	f^2	E_{3g}	0.000	0.000

Additional CI Calculations. The energy levels calculated with the two sets of IVOs are given in Table X. The energy order is the same except for a reversal of the f^2 A_{1g} and E_{3g} states. The u states above the first one, f $\rightarrow$ d A_{1u}, are lowered in energy by approximately 0.1 eV when π^{-1} orbitals are used in place of the f^{-1} orbitals.

Some investigation of the effect of double excitations was made. Adding $6d^2$ configurations had very little effect on the $5f^2$ states. Adding $\pi^2 \rightarrow \pi^{*2}$ configurations lowered the all of the $5f^2$ states by approximately 0.04 hartree and lowered all of the f $\rightarrow$ d states by approximately 0.02 hartree. It seems likely that further CI with the present set of active orbitals would not appreciably change the results and that substantial improvements in the calculated excitation energies would require a considerably larger number of MOs, including both g functions and more f functions on the uranium and more basis functions on the ligands. Such basis set expansion and increased CI length would likely improve the ligand description more than the uranium description and therefore result in reduced charge-transfer character in the lower electric-dipole-allowed states.

Conclusions. Ab initio calculations have been carried out on uranocene using core potentials and the corresponding spin–orbit operators. Moderate-size basis sets were used and spin–orbit CI calculations of moderate length were carried out. The results seem accurate enought to give valuable information on several aspects of the electronic structure and spectra of uranocene:

The uranium 6d orbitals play the primary role in covalent bonding between the metal and the ligands, while the 5f orbitals have a secondary role.

The electronic ground state of uranocene is E_{3g} ($|M_J| = 3$). The best simple description of the state is weak-field, LS-coupling, $5f^2$, $^3H_4$, $|M_J| = 3$, but significant deviations are evident in one of the 5f orbital splittings and in the amount of singlet character.

The characteristic green color of uranocene is due to transitions to E_{2u} and E_{3u} excited states, which are primarily 5f $\rightarrow$ 6d in nature but have some admixture of $\pi \rightarrow$ 6d charge-transfer character.

Detailed ultraviolet spectra would be useful because of the large number of predicted allowed transitions.

In addition to larger and more accurate CI calculations of excitation energies, it would be very useful to have calculations

of magnetic moments, transition moments, and spin densities using these wave functions.

Acknowledgment. This research was supported by the National Science Foundation under Grant CHE-8312286 and by Cray Research Inc. under a Cray Software Development Grant. We thank Dr. W. H. Miller and the Department of Chemistry, University of California, Berkeley, for their hospitality during the time that most of this work was carried out. Initial calculations were performed on the Cray X-MP/48 at the Pittsburgh Supercomputing Center and the Cray X-MP/24 at the Ohio Supercomputer Center. Most of the calculations were performed on the Cray X-MP/14 at the University of California, Berkeley, with a final set done on the Cray X-MP/416 at Cray Research Inc. We thank Dr. P. A. Christiansen for providing us with the uranium core potential and spin-orbit operators, and we thank Drs. N. Edelstein, A. Streitwieser, K. S. Pitzer, and K. N. Raymond for their help and advice.

Registry No. $U(C_8H_8)_2$, 11079-26-8.

Energetics and Hydration of the Constituent Ion Pairs of Tetramethylammonium Chloride

J. Kathleen Buckner and William L. Jorgensen*

Contribution from the Department of Chemistry, Purdue University, West Lafayette, Indiana 47907. *Received August 24, 1988*

Abstract: Statistical perturbation theory and Monte Carlo simulations have been utilized to obtain interionic potentials of mean force for the constituent ion pairs of tetramethylammonium chloride in dilute aqueous solution at 25 °C and 1 atm. For $(CH_3)_4N^+Cl^-$, a contact ion pair is found at an N-Cl distance of 5.0 Å and a broad minimum for the solvent separated form is centered near 7.5 Å. The two species are separated by a barrier of only 0.7 kcal/mol. From the calculated potential of mean force, the association constant for dilute aqueous $(CH_3)_4N^+Cl^-$ was determined to be 0.30 L/mol. For two chloride ions in water, a deep minimum is found at an interionic separation of 4.8-5.0 Å with a barrier to dissociation of ca. 6 kcal/mol. Though this result is qualitatively consistent with earlier findings, the possibility of a computational artifact is considered. The stability of the "solvent-bridged" ion pair can be attributed to the presence of three water molecules that simultaneously hydrogen bond to both chloride ions. In contrast, the approach of the other like ion pair, $(CH_3)_4N^+\cdots(CH_3)_4N^+$, is predicted to be purely repulsive. The energetic results are accompanied by details on the variation in solvation as a function of interionic separation.

The study of aqueous electrolyte solutions on a molecular level has revealed many properties of these systems not previously detected by theories that treat the solvent as a dielectric continuum. By examining the free energy as a function of the interionic distance or "potential of mean force" (pmf), statistical mechanical theories have been able to better describe the detailed mechanisms of ion pairing in solution. For example, integral equation studies of alkali halides in water have found oscillatory behavior in the pmfs for the anion-cation interactions.[1-3] A molecular dynamics calculation on aqueous NaCl[4] and a Monte Carlo study of aqueous *tert*-butyl chloride[5] showed the same behavior and clearly identified minima corresponding to contact and solvent-separated ion pairs. In the integral equation studies, cation-cation pmfs were also found to have modest minima that were not stabilized with respect to infinite separation.[1-3] Recently, an extended RISM treatment of dilute aqueous alkali halides[6] and a molecular dynamics simulation of two chloride ions in water[7,8] that used the same potential function model gave evidence for the existence of chloride ion pairs stabilized near contact in aqueous solution. The stability of these anionic pairs was attributed to bridging structures in which water molecules can hydrogen bond to both chloride ions simultaneously. Subsequently, the reference hypernetted chain (RHNC) approximation has been applied to aqueous ionic solutions at infinite dilution and finite concentrations.[9] The model consisted of hard sphere ions in a solvent of hard multipolar polarizable particles and corresponded to some alkali halides and $(C_2H_5)_4NBr$ in water. This study found contact and solvent-separated minima in the pmfs for the unlike-charged ions, though the solvent-separated minimum for Et_4NBr was very shallow. Attractive wells were also detected for the smaller like-charged ion pairs, both negative and positive. Due to the nature of the solvent model, the pmfs for the same size cations and anions are identical.

The association constant, K_a, is another property of salt solutions that can be better described with molecular models for the solvent. Bjerrum theory,[10] which has long been used to obtain association constants for infinitely dilute solutions, fails in many areas because it depends only on properties of the ions and on the dielectric constant of the solvent. For example, the theory predicts the association constants for tetraalkylammonium salts to decrease with increasing size in protic solvents. This trend is observed in alcoholic solvents, but the reverse trend occurs in water.[11] The reversal has been attributed to water structure-enforced ion pairing[12] in which larger, more hydrophobic ions are forced into the same cage by the solvent in order to decrease the disruption of the hydrogen-bonded network of water. A theoretical treatment of K_a that utilizes a molecular interpretation of the solvent should be able to explain such effects. In fact, an extended RISM study[13] of ion pairs in alcoholic solvents yielded trends in K_a's at infinite

(1) Patey, G. N.; Carnie, S. L. *J. Chem. Phys.* **1983**, *78*, 5183.
(2) Kusalik, P. G.; Patey, G. N. *J. Chem. Phys.* **1983**, *79*, 4468.
(3) Hirata, F.; Rossky, P. J.; Pettitt, B. M. *J. Chem. Phys.* **1983**, *78*, 4133.
(4) Berkowitz, M.; Karim, O. A.; McCammon, J. A.; Rossky, P. J. *Chem. Phys. Lett.* **1984**, *105*, 577. Belch, A. C.; Berkowitz, M.; McCammon, J. A. *J. Am. Chem. Soc.* **1986**, *108*, 1755. Karim, O. A.; McCammon, J. A. *J. Am. Chem. Soc.* **1986**, *108*, 1762.
(5) Jorgensen, W. L.; Buckner, J. K.; Huston, S. E.; Rossky, P. J. *J. Am. Chem. Soc.* **1987**, *109*, 1891.
(6) Pettitt, B. M.; Rossky, P. J. *J. Chem. Phys.* **1986**, *84*, 5836.
(7) Dang, L. X.; Pettitt, B. M. *J. Am. Chem. Soc.* **1987**, *109*, 5531.
(8) Dang, L. X.; Pettitt, B. M. *J. Chem. Phys.* **1987**, *86*, 6560.
(9) Kusalik, P. G.; Patey, G. N. *J. Chem. Phys.* **1988**, *88*, 7715.
(10) Davies, C. W. *Ion Association*; Butterworths Scientific Publications: London, 1962.
(11) Accascina, F.; Goffredi, M.; Triolo, R. *Z. Phys. Chem. Neu. Fol.* **1972**, *81*, 148.
(12) Diamond, R. M. *J. Phys. Chem.* **1963**, *67*, 2513.
(13) Hirata, F.; Levy, R. M. *J. Phys. Chem.* **1987**, *91*, 4788.

0002-7863/89/1511-2507$01.50/0